Pedological trends and implications for forest productivity in a Holocene soil chronosequence, Calvert Island, British Columbia, Canada

Authors: Nelson, Lee-Ann, Sanborn, Paul, Cade-Menun, Barbara J., Walker, Ian J., and Lian, Olav B.

Source: Canadian Journal of Soil Science, 101(4) : 654-672

Published By: Canadian Science Publishing

URL: https://doi.org/10.1139/cjss-2021-0033

NRC Research Press

ARTICLE

Pedological trends and implications for forest productivity in a Holocene soil chronosequence, Calvert Island, British Columbia, Canada

Lee-Ann Nelson, Paul Sanborn, Barbara J. Cade-Menun, Ian J. Walker, and Olav B. Lian

Abstract: Chronosequence studies of soil formation and ecosystem development provide important insights into the pathways and rates of change occurring on centennial and millennial time scales. In cool or temperate humid environments, Podzols are the predominant soil type formed under coniferous forests in coarse-textured parent material and have been a major focus of chronosequence studies. This study examined the rate and mechanisms of Podzol development and related forest productivity in a sand dune chronosequence in a hypermaritime climate in coastal British Columbia (BC). The sequence spans 10 760 ± 864 yr over eight sites and is the first documented chronosequence in coastal BC to span most of the Holocene Epoch. Soil samples from each genetic horizon were analyzed for bulk density, pH and concentrations of total carbon (C), pyrophosphate- and oxalate-extractable aluminum (Al) and iron (Fe), and total elements. Within ~3500 yr, a mature Podzol had formed, with cemented horizons (ortstein and placic) present. Organo-metallic complexation appeared to be the dominant mechanism involved in podzolization. Despite a mild, moist climate conducive to chemical weathering, all soils had similarly low values for the chemical index of alteration, suggesting that congruent dissolution of primary minerals may be occurring. Ecosystem retrogression is apparent in the latter stages of the chronosequence — a phenomenon not previously documented in coastal BC. Further research is needed to examine the interactions of nutrient limitation, soil physical barriers, and other possible drivers of ecosystem retrogression.

Key words: Podzols, chronosequence, ecosystem retrogression, chemical index of alteration, British Columbia, soil genesis.

Résumé : Étudier la séquence chronologique de la genèse d'un sol et du développement d'un écosystème nous procure d'importants indices sur la façon dont les changements surviennent et la vitesse à laquelle ils le font au long des siècles et des millénaires. Dans les climats frais ou tempérés-humides, le podzol est le sol prédominant qui se forme dans les forêts de conifères poussant sur un matériau originel à texture grossière. On s'est beaucoup intéressé à ce type de sol dans les études sur la chronoséquence. Les auteurs ont examiné la vitesse et les mécanismes de développement d'un podzol et la productivité de la forêt qu'il supporte dans la chronoséquence d'une dune de sable située dans sur la côte de la Colombie-Britannique (C.-B.), dans un climat hypermaritime. La séquence s'étend sur 10 760 ± 864 ans et huit sites, et est la première chronoséquence de la côte de la C.-B. s'étalant sur la majeure partie de l'Holocène à être documentée. Les auteurs ont déterminé la masse volumique apparente, le pH ainsi que la concentration totale de carbone (C), d'aluminium extractible au pyrophosphate et à l'oxalate (Al) et de fer, de même que la teneur en oligoéléments des échantillons prélevés dans chaque horizon génétique. Un podzol mature s'est développé en l'espace d'environ 3 500 ans, avec des horizons cimentés (orstein et placique). La formation de complexes organométalliques semble être le principal mécanisme à son origine. Malgré le temps doux et humide, propice à la lixiviation, les sols avaient tous un faible indice d'altération

Received 31 March 2021. Accepted 3 June 2021.

L.-A. Nelson and P. Sanborn. University of Northern British Columbia, 3333 University Way, Prince George, BC V2N 4Z9, Canada.

B.J. Cade-Menun. Swift Current Research and Development Centre, Agriculture & Agri-Food Canada, Swift Current, SK 9H 3X2, Canada.

I.J. Walker. Department of Geography, Division of Mathematical, Life and Physical Sciences, University of California Santa Barbara, Santa Barbara, CA 93106, USA.

O.B. Lian. School of Land Use and Environmental Change, University of the Fraser Valley, 33844 King Road, Abbotsford, BC V2S 7M8, Canada.

Corresponding author: Paul Sanborn (email: Paul.Sanborn@unbc.ca).

chimique, signe qu'il pourrait y avoir eu parallèlement dissolution des principaux minéraux. La rétrogression de l'écosystème est manifeste dans les derniers stades de la chronoséquence – un phénomène qui n'avait pas été rapporté précédemment sur la côte de la C.-B. Il faudrait entreprendre des recherches plus poussées pour examiner comment la concentration restreinte d'oligoéléments, les obstacles physiques dans le sol et d'autres facteurs éventuels ont interagi pour entraîner la rétrogression de l'écosystème. [Traduit par la Rédaction]

Mots-clés : podzols, chronoséquence, rétrogression de l'écosystème, indice d'altération chimique, Colombie-Britannique, pédogenèse.

Introduction

Chronosequence studies of soil formation and ecosystem development involve substitution of space for time, using arrays of sites with similar parent geological material, climate, topography, and biotic influences. Such studies provide important insights into the pathways and rates of change occurring on centennial and millennial time scales (Walker et al. 2010). As the predominant soil type formed under coniferous forests in coarse-textured parent geological material in cool or temperate humid environments (McKeague et al. 1983), Podzols and their pedogenesis have been a major focus of chronosequence studies, both internationally (Sauer et al. 2008) and in Canada (Sanborn 2016). Podzols are characterized by the accumulation of amorphous organic matter (OM) and (or) the enrichment of iron (Fe) and aluminum (Al) in the B horizon (Sanborn et al. 2011). Cementation, in the form of ortstein and placic horizons, is an accessory feature of many Podzols (Sanborn et al. 2011), and their formation can modify ecologically significant soil attributes such as strength and hydraulic conductivity.

Longer-term (millennial) chronosequence studies require settings where catastrophic disturbance has been largely absent since initial site establishment, allowing examination of soil and ecosystem attributes at, and after, the maximal biomass phase of succession. Without catastrophic disturbance, the maximal biomass phase in late primary or secondary succession cannot persist indefinitely, and is followed by a decline in primary productivity (Wardle et al. 2004). This decline phase is known as ecosystem retrogression, and it is often attributed to a decline in phosphorus (P) availability to aboveground biomass (Walker and Syers 1976; Wardle et al. 2004). The most common metric used to determine if retrogression has occurred is tree basal area (BA; Westman and Whittaker 1975; Wardle et al. 2004; Peltzer et al. 2010). Accompanying a decline in aboveground biomass, there is also a marked shift in plant communities with age, with more nutrient-demanding species on younger sites and more stress-tolerant, slow-growing species on older sites (Jenny et al. 1969; Coomes et al. 2005; Eger et al. 2011).

Research in Canada conducted in diverse environments has documented that Podzol formation can require, at one extreme, more than 12 000 yr under subarctic conditions (LaFortune et al. 2006). Much faster pedogenesis occurs in moister, milder temperate rainforests in coastal British Columbia (BC), with Podzol formation occurring in under 400 yr in the well-studied Cox Bay chronosequence on western Vancouver Island (Singleton and Lavkulich 1987*a*, 1987*b*). Longer-duration chronosequence studies are needed to address the full scope of Holocene soil formation and its accompanying ecological transformations in coastal BC. However, only preliminary work has occurred in two separate areas (Fig. 1*a*): (*i*) the Brooks Peninsula chronosequence on the south coast of BC (northwestern Vancouver Island), which spans approximately 8000 yr, albeit with poorly constrained ages (Maxwell 1997); and (*ii*) the Naikoon chronosequence on the north coast of BC (Graham Island, Haida Gwaii), which spans about 6500 yr with a well-constrained chronology (Wolfe et al. 2008).

Western North American coastal temperate rainforests extend from northern California to southeast Alaska, and soil formation in these ecosystems is expected to be rapid because of high rainfall. In turn, a variety of genetic soil types can result, depending on the topography, water table position, and parent materials (Banner et al. 2005; D'Amore et al. 2015). In these coastal temperate rainforests, nutrient-poor soils are common due to high leaching, resulting in a wide range of ecosystem productivity, from productive upland forests to bog forests to blanket bogs (Banner et al. 2005). In forested soils of this region, imperfectly drained Podzols and Folisols with thick forest floors (FF) are dominant, but other Organic soils can also form in depressions (Banner et al. 2005).

There is a limited body of existing research on soil chronosequences in BC, which highlights the need for more studies examining soil development during the Holocene Epoch. Such research also provides an opportunity to explore accompanying changes in ecosystem development, such as retrogression (Sanborn 2016). The primary objective of this study was to examine the rate of Podzol development along a Holocene soil chronosequence developed on aeolian dunes found on Calvert Island, BC in the Coastal Western Hemlock (CWH) biogeoclimatic zone. The second objective was to examine soil chemical and morphological changes over time in relation to mechanisms of Podzol formation. In addition, we hypothesized that prolonged weathering would result in the loss of nutrients that would affect forest productivity. Thus, the third objective of the study was to explore the interaction of soil development and forest

Fig. 1. (*a*) Location of Calvert Island on the central coast of British Columbia, Canada in relation to the Brooks Peninsula, Cox Bay, and Naikoon soil chronosequences; and (*b*) detailed map of study sites on northwestern Calvert Island, BC, Canada illustrating the locations of the stabilized aeolian dunes and prograding foredune locations that were sampled for this study (adapted from Neudorf et al. 2015 and Nelson et al. 2020). Note that sampling sites are denoted with a red circle. [Colour online.]

(a)

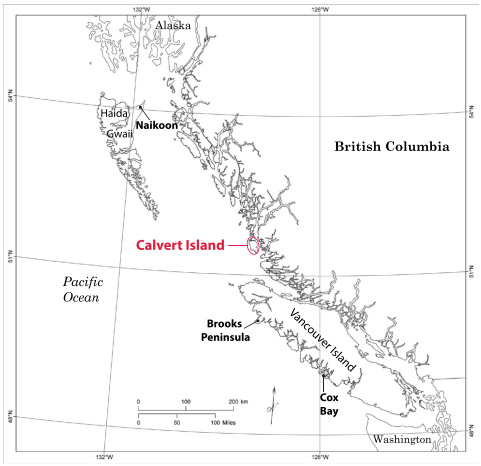

(b)

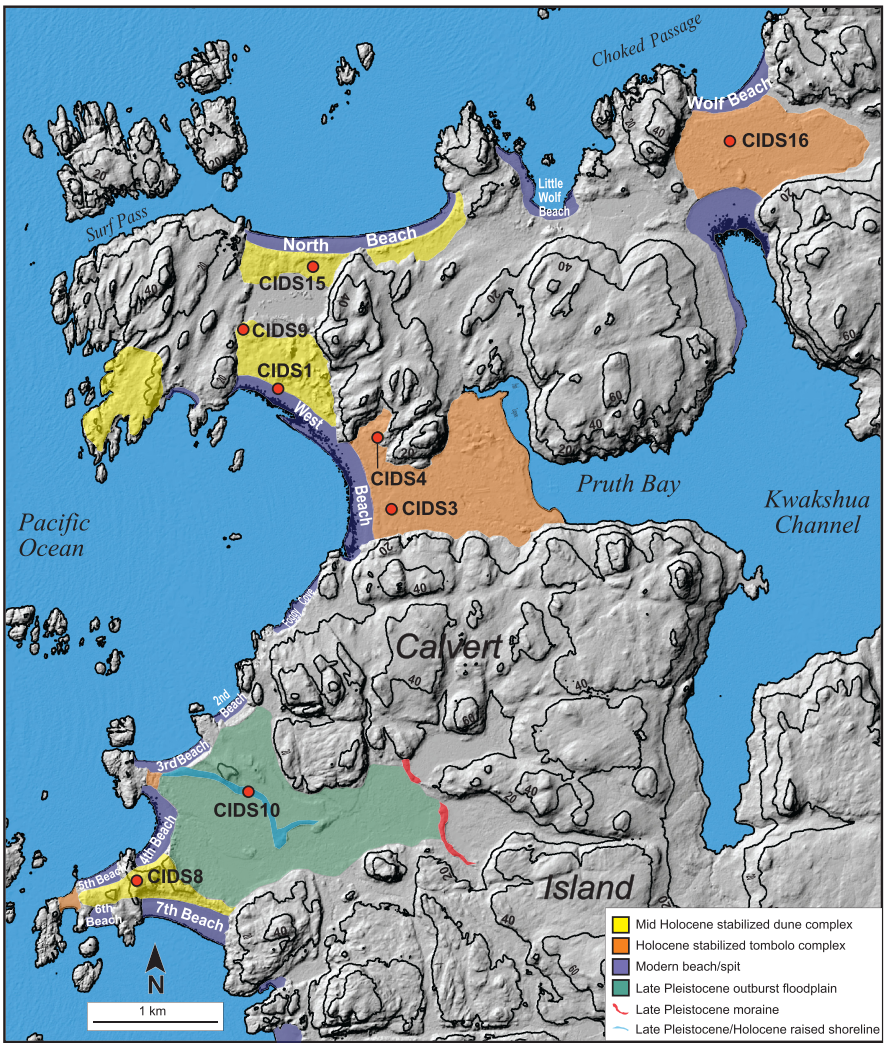

productivity over time to determine if ecosystem retrogression is occurring on the oldest sites.

Materials and Methods

Study area

The study area was located on northwestern Calvert Island on the central coast of BC, situated approximately 80 km north of Vancouver Island (Fig. 1*a*). Calvert Island is situated in the Hecate lowlands ecoregion in the CWH biogeoclimatic zone (Hebda 1995), Very Wet Hypermaritime subzone, and Central variant (CWHvh2; Banner et al. 2005). Calvert Island has a temperate, humid climate (Supplementary Table S1[1]; MOE 2016). The characteristic tree species within the CWHvh2 variant are western redcedar (*Thuja plicata* Donn ex D. Don), western hemlock [*Tsuga heterophylla* (Raf.) Sarg.], and yellow cedar (*Callitropsis nootkatensis* D. Don), and the characteristic shrubs are false azalea (*Menziesia ferruginea* Sm.), salal (*Gaultheria shallon* Pursh), and Alaskan blueberry (*Vaccinium alaskaense* Howell; Banner et al. 1993). The Calvert Island chronosequence has a variety of specific site units within the CWHvh2 variant that also have Sitka spruce [*Picea sitchensis* (Bong.) Carr.] and shore pine (*Pinus contorta* Douglas ex Loudon var.*contorta*).

Studies from Haida Gwaii, about 250 km to the northwest, suggest that the Cordilleran Ice Sheet advanced over Calvert Island between 30 and 22 ka (Mathewes and Clague 2017), whereas a local study indicates that it had begun to retreat from Calvert Island by ~18 ka (Darvill et al. 2018). Calvert Island was at least locally forested prior to 14.2 cal ka, when a cooling climate resulted in a short-lived glacial advance that ended by about 13.8 cal ka when relative sea level (RSL) dropped to a position slightly lower than present (Eamer et al. 2017, 2018). During that time, cold and dry conditions facilitated the development of significant dune fields along the coastal regions of Calvert Island, which had begun to stabilize by about 11 cal ka (Eamer et al. 2018). The period from about 8.5 until 0.4 cal ka saw the development and stabilization of extensive low-lying sandy landscapes (isthmuses), such as those that formed North and West beaches, and closed off Kwakshua Channel forming Pruth Bay (Eamer et al. 2018). Episodes of destabilization of sedimentary landforms as a result of fire have also been recorded on Calvert Island during postglacial time (Hoffman et al. 2016), and some events may have been associated with human presence in the area over the last 1000 yr (Stafford and Christensen 2014).

Calvert Island has a distinctive sea level history, whereby the RSL has remained within 1–2 m of the current sea level for the past 15 000 yr, following the retreat of the short-lived re-advanced lobe of the Cordilleran Ice Sheet mentioned earlier (McLaren et al. 2014; Eamer et al. 2017). Broader empirical evidence of RSL trends in the region suggests that the study site is located along a sea-level "hinge" where RSL changed very little over the Holocene due to the counteracting effects of isostatic rebound of Calvert Island coinciding with post-glacial eustatic adjustments (McLaren et al. 2014; Shugar et al. 2014; Eamer et al. 2017).

This study focuses on an array of sites developed on sandy landforms that are composed predominantly of quartz sand (Neudorf et al. 2015). Eight aeolian sand dune locations were examined in this study, with ages ranging from a modern, established foredune [~0 yr before 2012, when samples were collected and dated (0 a)] to a stabilized, relict sand dune dated to approximately 10 760 ± 864 a (Supplementary Table S2[1]; Fig. 1*b*). These landforms were dated by optically stimulated luminescence (OSL) dating, which estimates the last time that mineral grains were exposed to sunlight (Neudorf et al. 2015). Prior to this study, these dune sites were visited to verify the extent to which they met key requirements for a soil chronosequence, including progressive soil development, minimal disturbance, similar soil parent material, and topography (Jenny 1941; Walker et al. 2010), and sufficient area to accommodate two replicate sampling locations. The maximum separation of these sites was approximately 8 km, so it would be reasonable to assume that similar climatic conditions would have existed across the sequence at any given time.

All parent material (C) and (or) deep transitional (BC) horizons when the C horizon was not reached were comparable in physical, chemical, and morphological characteristics (e.g., no differences in carbonate content, texture, colour; Nelson 2018). Drainage appeared to be similar across all sites, aside from those where cemented horizons impeded water flow, which is an expected stage of soil development in this portion of the CWH zone (Banner et al. 2005). Seepage was identified on the 3588, 4198, and 7236 a sites, due to the degree of cementation. All sites lie within 35 m of sea level, with the two sites at the lower end of the elevation range (105 and 7236 a) experiencing somewhat poorer drainage conditions (Supplementary Table S2[1]), although their relative degrees of soil development were comparable to those of other sites of similar age. Although there have been significant changes in climate during the past 11 000 a, palaeobotanical records show that current early successional plant species (e.g., coastal strawberry; *Fragaria chiloensis* ssp. *Pacifica*) were present on Calvert Island when the oldest site was formed (10 760 ± 864 a), and tree species currently dominant on Calvert Island [e.g., Sitka spruce, red alder (*Alnus rubra* Bong.) and redcedar] were also present by 840 a (Eamer 2017). The successional stage within the 605 a site was not consistent due to downed trees and large woody debris within the soil

[1]Supplementary data are available with the article at https://doi.org/10.1139/cjss-2021-0033.

profile (replicate B); however, the degree of soil development and horizonation were not significantly disrupted and were comparable to replicate A. On balance, the Calvert Island sites collectively meet the requirements for a chronosequence study (Jenny 1941; Walker et al. 2010) and, as such, they provide adequate potential to yield insights into long-term soil and ecosystem development in this region.

Site selection and sample collection

Two sampling locations (designated as replicates A and B) on each sand dune were selected in stable, representative landscape positions to capture the variability of soil development within the dune. When possible, sampling locations were chosen on upland positions that were flat to gently sloping, with well- to moderately well-drained conditions. Elevation was estimated from a 3 m digital elevation model derived from aerial LiDAR (Supplementary Table S2[1]).

Horizons were designated and each pedon was described and classified according to Canadian System of Soil Classification (SCWG 1998) and Ministry of Forests and Range (2010). Samples were collected from each soil genetic horizon. All soil samples were air-dried, ground using a mortar and pestle or coffee grinder, and sieved to 2 mm. Soil mass per unit area was determined for individual horizons, except where multiple thin horizons were captured in a single core sample. For organic horizons, a cordless drill with a steel coring tube was utilized to sample the entire FF to calculate its mass per unit area (Nalder and Wein 1998). When the organic horizon thickness was greater than the length of the coring tube, a slide hammer and coring ring were used to take bulk density samples from the side of the pit, whereas for uncemented mineral soil horizons, a slide hammer corer was utilized on a ledge of undisturbed soil (Blake and Hartge 1986). For cemented soil horizons, the clod method was used to determine soil bulk density (Blake and Hartge 1986).

Soil characterization

Samples were sent to Maxxam Laboratories (Burnaby, BC) for particle size analysis via the pipette technique (Gee and Bauder 1986) after pre-treatment with hydrogen peroxide and citrate–dithionite–bicarbonate for removal of OM and iron oxides, respectively. Samples were sent to the BC MECCS Analytical Chemistry Services Laboratory (Victoria, BC) for chemical analysis, including total carbon (C) and nitrogen (N), exchangeable cations [calcium (Ca^{2+}), magnesium (Mg^{2+}), sodium (Na^{2+}), and potassium (K^{+})], pH in 0.01 mol·L^{-1} calcium chloride ($CaCl_2$), and total elemental analysis. Sample analysis is described in detail in Nelson (2018) and Nelson et al. (2020).

Sodium pyrophosphate (0.1 mol·L^{-1}) and acidified ammonium oxalate (0.2 mol·L^{-1}) were used to extract Fe, Al, and silicon (Si) from mineral samples, followed by inductively coupled plasma optical emission spectroscopy (McKeague and Day 1966; Courchesne and Turmel 2008). Pyrophosphate-extractable Fe (Fe_p) and Al (Al_p) represent organically complexed Fe and Al, whereas oxalate-extractable Fe (Fe_o) and Al (Al_o) represent amorphous and organically complexed Fe and Al. The difference between oxalate- and pyrophosphate-extractable Fe and Al provides an indication of the quantity of amorphous forms (Farmer and Fraser 1982; Gustafsson et al. 1995). The estimated concentration of allophanic materials (non-crystalline aluminosilicates) of each horizon was calculated using the method developed by Parfitt (1990).

Aboveground biomass measurements

Basal area was used as a surrogate method to assess aboveground tree biomass, and it was determined using an adapted form of the National Forest Inventory protocol (NFI 2008). Due to the variable widths of the dunes, the narrowest dune was used to determine the maximum radius for a fixed-radius plot allowing for replication. Therefore, a fixed-radius plot of 3.99 m was used. Basal area determination was replicated three times per site to encompass the variability of the aboveground biomass, and locations ran lengthwise across foredunes and were randomly spread on all other dunes. All trees over 9 cm diameter at breast height (DBH) were measured to one mm, whereas trees less than 9 cm DBH were tallied according to size class (0–2.9, 3.0–5.9, and 6.0–8.9 cm DBH).

Tree foliage sampling and analysis

Foliage was collected from western redcedar and western hemlock growing within 5 m of each pedon when present using an adapted Ballard and Carter (1986) method. Foliage samples were pruned by hand when possible and intact, green foliage was retrieved from the ground if hand sampling was not feasible. Sampling could not be limited to current year foliage because it was not possible to separate needle cohorts reliably on slow-growing, stunted trees on the older sites. Foliage samples were oven-dried at 60 °C, ground using a coffee grinder, and stored at room temperature in sealed plastic bags prior to analysis. Individual foliage samples were analyzed for total C, N, and P as described in Nelson (2018) and Nelson et al. (2020).

Chemical weathering index

The chemical index of alteration (CIA) provides an indication of the degree of weathering of a soil horizon by comparing the molar ratio of a relatively immobile element, Al, to the sum of Al and more mobile elements (Ca, Na, and K), expressed in oxide form (eq. 1; Nesbitt and Young 1982). Total element concentrations were obtained by lithium metaborate fusion using a Claisse M4 Fluxer (Claisse 2003) [see Nelson (2018) for more details]. The CIA values from the deepest C horizons on

Table 1. Pedon classification, site series, and soil morphology including bulk density (Db) and pH in calcium chloride ($CaCl_2$).

Landform age (a), Site No., Replicate (A or B), Classification[a]	Site series (BEC): dominant plant species[b]	Landform type	Horizons[c]	Depth (cm)	Colour (moist)	Structure[d]	Texture[e]	Db ($g \cdot cm^{-3}$)	pH (in $CaCl_2$)
0, CIDS1, Replicate A, CU.R	Modern dune: dune grass	Established foredune	C	0–27	5Y 6/2	SG	S	1.36	7.8
			Ahb	27–34	2.5Y 4/2	SG	S	1.28	7.6
			C2	34–62	5Y 6/2	SG	S	1.18	7.9
			Ahb2	62–67	2.5Y 5/2	SG	S	1.17	7.8
			BC	67–116	5Y 5.5/1	SG	S	1.17	7.9
0, CIDS1, Replicate B, CU.R	Modern dune: dune grass	Established foredune	C	0–13	2.5Y 6/2	SG	S	1.33	7.5
			Ahb	13–18	5Y 3/2	MA, SG	S	1.16	7.0
			BC	18–92	5Y 6/2	SG	S	1.25	7.7
			C2	92–111+	5Y 7/1	SG	S	1.25	7.7
105 ± 15, CIDS3, Replicate A, E.DYB	15 Ss:Hw/Dr/Ss	Stabilized, forested foredune	Organic horizon: S/L 28-26/Fm 26-22/Hw 22-0						
			Ae	0–3	2.5Y 5/2	SG	S	1.20	3.7
			Bmj	3–58	10YR 4/3	SG	S	1.25	4.4
			BC	58–93+	2.5Y 4/3	SG	S	1.37	4.4
105 ± 15, CIDS3, Replicate B, E.DYB	15 Ss:Hw/Dr	Stabilized, forested foredune	Organic horizon: S/L 37-35/Fm 35-33/Hw 33-0						
			Ae	0–3	2.5Y 5/2	SG	S	1.20	3.7
			Bhj	3–26	10YR 4/4	SG	S	1.22	4.0
			Bm	26–55	2.5Y 4/3	SG	S	1.37	4.3
			BC	55–120+	2.5Y 5/3	SG	S	1.46	4.4
139 ± 17, CIDS4, Replicate A, E.DYB	01 CwHw:Ss/Hw/Cw	Stabilized, forested foredune	Organic horizon: S/L 9-8/Fa 8-7/Hh 7-0						
			Ae	0–3	2.5Y 5/2	SG	S	0.98	3.3
			Bhj	3–23	10YR 4/3	SG	S	1.25	4.2
			Bm	23–73	2.5Y 5/3	SG	S	1.37	4.7
			BC	73–111+	2.5Y 6/8	SG	S	1.25	5.0
139 ± 17, CIDS4, Replicate B, E.DYB	01 CwHw:Hw/Ss	Stabilized, forested foredune	Organic horizon: S/L 10-8/Fm 8-6/Hh 6-0						
			Ae	0–5	10YR 4/1	SG	S	0.93	3.7
			Bhj	5–19	10YR 3/4	SG	S	1.20	4.0
			Bm	19–64	2.5Y 6/3	SG	S	1.31	4.6
			BC	64–103+	2.5Y 6/3	SG	S	1.36	4.9
605 ± 50, CIDS9, Replicate A, E.DYB	03a CwYc:Hw/Dr	Established, forested dune	Organic horizon: S/L 25-23/Fm 23-18/Hh 18-5/Hw 5-0						
			Ae	0–6	5Y 7/1	SG	S	0.96	3.7
			Bhj	6–36	10YR 3/2	MA, SG	S	1.26	4.1
			Bhc	36–39	7.5YR 2.5/3	MA	S	1.26	4.0
			Bmj	39–90	10YR 3/	MA, SG	S	1.35	4.3
			BC	90–112+	2.5Y 4/4	MA	S	1.33	4.4

Table 1. (*continued*).

Landform age (a), Site No., Replicate (A or B), Classification[a]	Site series (BEC): dominant plant species[b]	Landform type	Horizons[c]	Depth (cm)	Colour (moist)	Structure[d]	Texture[e]	Db ($g \cdot cm^{-3}$)	pH (in $CaCl_2$)
605 ± 50, CIDS9, Replicate B, E.DYB	03a CwYc:Cw/Dr	Established, forested dune	Organic horizon: L 4-3/Fm 3-1/Hi 1-0						
			Ahe	0–13	10YR 4/2	SG	S	0.86	3.4
			Hwb	13–33	7.5YR 2.5/1	—	—	0.10	3.2
			Bm	33–58	2.5Y 5/4	MA	S	1.14	3.9
			Bhjcj	58–113	10YR 3/2	MA	S	1.14	4.1
3588 ± 303, CIDS8, Replicate A, OT.HP	14 Ss:Hw/Cw/Ss	Forested, dune-capped tombolo	Organic horizon: L 37-34/Fm 34-15/Hw 15-0						
			Ahe	0–6	10YR 5/4	MA	LS	1.42	3.8
			Ae	6–25	2.5Y 6/2	SG	S	1.42	3.9
			Bhc	25–43	10YR 2/2	MA	S	1.56	4.3
			Bfc1	43–45	2.5YR 2.5/3	MA	S	1.76	4.5
			Bm1	45–65	7.5YR 3/2	SG	S	1.42	4.4
			Bfc2	65–67	5YR 3/4	MA	S	1.76	4.5
			Bm2	67–95	10YR 3/4	MA	S	1.41	4.6
			BC	95–163+	2.5YR 5/4	SG	S	1.41	4.7
3588 ± 303, CIDS8, Replicate B, OT.HP	14 Ss:Hw/Ss	Forested, dune-capped tombolo	Organic horizon: L 28-27/Fa 27-10/Hw 10-0						
			Ae	0–22	2.5Y 6/2	SG	S	0.96	3.6
			Bhc	22–57	5YR 2.5/1	MA	S	1.24	4.1
			Bfcj1	57–58	7.5YR 2.5/2	MA	S	1.29	4.7
			Bh	58–72	7.5YR 3/2	MA	S	1.29	4.5
			Bhcj2	72–106	5YR 2.5/1	MA	S	1.29	4.4
4198 ± 332, CIDS15, Replicate A, OT.HP	01 CwHw:Hw/Ss/Cw	Relict, forested foredune	Organic horizon: S/L 20-18/Fm 18-14/Hh 14-0						
			Ae	0–4	10YR 4/1	MA	SL	0.68	3.2
			Ahe	4–12	10YR 3/2	MA	SL	0.68	3.2
			Bhc	12–21	10YR 2/1	MA	LS	1.29	3.4
			Bfcj	21–23	2.5YR 2.5/3	MA	S	1.64	4.3
			Bmcj	23–49	10YR 4/6	MA	S	1.66	4.6
			BC	49–103+	2.5YR 5/4	SG	S	1.28	5.1
4198 ± 332, CIDS15, Replicate B, OT.HP	01 CwHw:Hw/Cw/Yc	Relict, forested foredune	Organic horizon: S/L 18-16/Fm 16-13/Hh 13-0						
			Ae	0–9	10YR 4/3	SBK	L	0.68	3.3
			Ahe	9–14	10YR 3/1	MA	LS	0.68	3.4
			Bhc1	14–28	10YR 2/1	MA	S	1.25	3.6
			Bhc2	28–38	10YR 3/6	MA	S	1.24	4.2
			Bh	38–43	7.5YR 2.5/2	MA	S	1.24	4.2
			Bfc	43–45	2.5YR 2.5/4	MA	S	1.63	4.4
			Bm	45–128+	2.5Y 5/4	MA	S	1.32	4.8

Table 1. (*concluded*).

Landform age (a), Site No., Replicate (A or B), Classification[a]	Site series (BEC): dominant plant species[b]	Landform type	Horizons[c]	Depth (cm)	Colour (moist)	Structure[d]	Texture[e]	Db ($g \cdot cm^{-3}$)	pH (in $CaCl_2$)
7236 ± 546, CIDS16, Replicate A, HU.FO	11 CwYc:Cw/Hw/Yc/Pc	Forested foredune	Organic horizon: S/L 0-3/Fa 3-8/Hw 8-35/Oh 35-55						
			Bhc	55–64	5YR 2.5/2	MA	S	1.18	3.8
			Bhcj	64–80	10YR 3/3	MA	S	1.04	4.3
			Bfc	82–81	5YR 3/4	MA	S	1.58	4.3
			Bm	81–136+	10YR 4/4	MA	S	1.31	4.6
7236 ± 546, CIDS16, Replicate B, HU.FO	11 CwYc:Cw/Hw/Yc/Pc	Forested foredune	Organic horizon: S/L 0-4/Fm 4-12/Hw 12-45/Oh 45-63						
			Bhc	63–85	7.5YR 2.5/2	MA	S	1.31	3.3
			Ae	85–86	2.5Y 4/2	SG	S	1.25	3.9
			Bmcj	86–103	7.5YR 2.5/3	MA	S	1.25	3.6
10760 ± 864, CIDS10, Replicate A, P.HP	11 CwYc:Cw/Yc/Hw/PC	Relict, stabilized, forested dune	Organic horizon: Lv 28-27/Fm 27-24/Hh1 24-10/Hh2 10-0						
			Bhcj	0–10	10YR 2/1	MA	LS	0.87	3.2
			Ae	10–12	10YR 7/1	SG	—	0.87	4.9
			Bfc	12–15	5YR 4/4	MA	S	1.49	4.6
			Bmcj1	15–70	2.5Y 7/3	MA	S	1.27	5.1
			BCg1	70–138	2.5Y 7/3	MA	S	1.27	5.3
10760 ± 864, CIDS10, Replicate B, E.DYB	11 CwYc:Cw/Hw/Pc	Relict, stabilized, forested dune	Organic horizon: S/L 28-25/Fm 25-20/Hh1 20-14/Hh2 14-0						
			Bhc	0–7	10YR 2/1	MA	LS	0.96	3.4
			Ae	7–10	2.5Y 5/3	SG	S	0.96	3.8
			Bfc	10–13	5YR 4/6	MA	S	1.23	4.6
			Bmcj	13–33	10YR 5/8	MA	S	1.23	5.3
			BC	33–90+	5Y 6/2	MA	S	1.31	5.5

[a]Soil classification according to Soil Classification Working Group (SCWG 1998): Cumulic Regosol (CU.R), Eluviated Dystric Brunisol (E.DYB), Ortstein Humic Podzol (OT.HP), Humic Folisol (HU.FO), and P.HP (Placic Humic Podzol).

[b]Tree species (Banner et al. 1993): red alder (Dr), western redcedar (Cw), yellow cedar (Yc), western hemlock (Hw), and shore pine (Pc).

[c]Horizon notation according to Soil Classification Working Group (SCWG 1998; https://sis.agr.gc.ca/cansis/taxa/cssc3/chpt02_a.html#soilhorizons) and Ministry of Forests and Range (2010).

[d]Structure (SCWG 1998): single grain (SG), massive (MA), and subangular blocky (SBK).

[e]Texture (Gee and Bauder 1986): sand (S), sandy loam (SL), and loamy sand (LS).

the youngest site (replicate A, C3 horizon; replicate B, C2 horizons) were used as the assumed parent geological material CIA value for comparison purposes. Calcium was corrected (CaO*) to represent only Ca occurring in silicate minerals (Nesbitt and Young 1982).

$$(1) \qquad \mathrm{CIA} = \left(\frac{\mathrm{Al_2O_3}}{\mathrm{Al_2O_3} + \mathrm{CaO^*} + \mathrm{Na_2O} + \mathrm{K_2O}}\right) \times 100\%$$

Data analysis

Means and standard deviations were calculated for the replicate pedons to examine variability within a dune. Because each profile had unique genetic horizons and associated thicknesses, a weighted average using bulk density and mass per area measurements were calculated for all horizon types (FF, A, and B) for all data unless otherwise noted. All depth graphs were created using weighted averages for 10 cm increments.

Linear and non-linear regression analyses were performed on the mass of total C to 1 m depth using STATA 14 IC. Akaike's information criteria was used to determine which model fitted best, and only models that realistically represented pedogenic processes were used (Schaetzl et al. 1994).

Results

Soil morphology

Pedons on the youngest site (~0 a), an established foredune, were classified as Cumulic Regosols (CU.R; Table 1; Fig. 2; SCWG 1998). Within 105 ± 15 to 139 ± 17 a on stabilized, forested foredunes, bleached eluvial horizons had formed, and 28–37 cm of FF had accumulated (Table 1; Fig. 2). Pedons on these sites were classified as Eluviated Dystric Brunisols (E.DYB). After 605 ± 50 a, pedons on an established, forested dune with evidence of tree throw had developed diagnostic organic-enriched B horizons and ortstein cemented horizons. Pedons on the 605 a site were classified as E.DYB (Table 1).

Within 3588 ± 303 a, mature Podzols had formed on a forested, dune-capped tombolo landform, which is a narrow isthmus that connects the main island to smaller proximal island(s) (see Eamer et al. 2018). Two types of cemented horizons (ortstein and placic) had formed, and pedons met the criteria for an Ortstein Humic Podzol (OT.HP; Table 1; Fig. 2). The pedons at the 4198 a site exist on a relict (stabilized, inactive) forested foredune and were also classified as OT.HP. On the 7236 a site on a forested foredune, both pedons were classified as Humic Folisols (H.FO) due to FF thickness but morphologically resembled an Orthic Humic Podzol (O.HP; replicate A) and an Ortstein Humic Podzol (OT.HP; replicate B), respectively. Replicate B was sampled at the original site where the OSL sample was obtained, and the depth of soil development was considerably greater than for any other pedon, with the Bh horizon transitioning to a BC at 2.23 m (Table 1). The two pedons at the 10 760 a site, a dune occupied by bog forest, were morphologically similar, but differences in B horizon thickness placed them in different soil orders: Placic Humic Podzol (P.HP) and E.DYB (Table 1; SCWG 1998). The FF at this site had a distinctive light brown humic horizon (Hh2) beneath the much darker brown organic Hh1 horizon (Table 1; Fig. 2).

Fig. 2. Representative soil profiles from the youngest to the oldest sites on the Calvert Island Chronosequence, BC. The youngest site (0 a, CIDS1A) is a Cumulic Regosol, the 139 a (CIDS4B) is an Eluviated Dystric Brunisol, the 3588 a (CIDS8B) is an Ortstein Humic Podzol, and the 10 760 a (CIDS10A; knife handle is 11 cm) sites is a Placic Humic Podzol. [Colour online.]

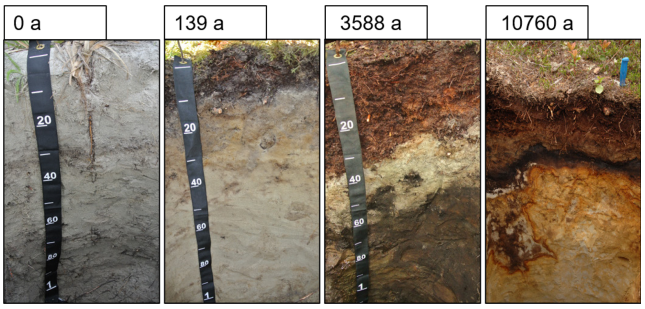

Most soil horizons remained structureless with increasing age; however, there was a shift from single grained to massive as cementation developed. Soil textures other than sand were present in some Ae and Ahe horizons after 3588 ± 303 a (Table 1). The average concentration of clay in all horizons is 2.2% [standard deviation (SD) 1.8] and ranged from <0.01% clay in the C horizons of the youngest site to 9.1% clay in the Ahe horizon of the 7236 a site (Supplementary Table S3[1]). Root restriction and seepage from temporary perched water tables above cemented horizons were evident at most sites older than 3500 a (Nelson 2018). Evidence of fire was prevalent in the form of charcoal in at least one horizon (typically the lowest organic or first mineral horizon) in all sites older than 3500 a and fires scars on living trees on all sites older than 7000 a.

Soil chemical properties

The greatest decline in pH was between 0 and 105 ± 15 a in all horizons, corresponding to Ae development and FF accumulation, followed by little change in the remainder of the chronosequence (Table 1). The pH within the FF decreased with depth (Nelson et al. 2020). The FF maintained appreciable concentrations of exchangeable base cations with increasing age, particularly on the 3588 and 4198 a sites (Fig. 3*a*). The greatest base cation concentration in the A horizon was found on the youngest site (~0 a), and the least was on the oldest site (10 760 a; Fig. 3*b*). The concentration of base cations was least in the B horizon compared with all other horizon types (Fig. 3*b*).

Fig. 3. Average sum of barium chloride-extractable base cations (Ca^{2+}, Mg^{2+}, Na^{+}, and K^{+}) of each soil horizon with one standard deviation indicated by the error bars; forest floor (FF; *a*), A and B mineral horizons (*b*; $n = 2$). (Note that the 0 a site did not have an FF or a B horizon, so only data for the BC horizon appear.)

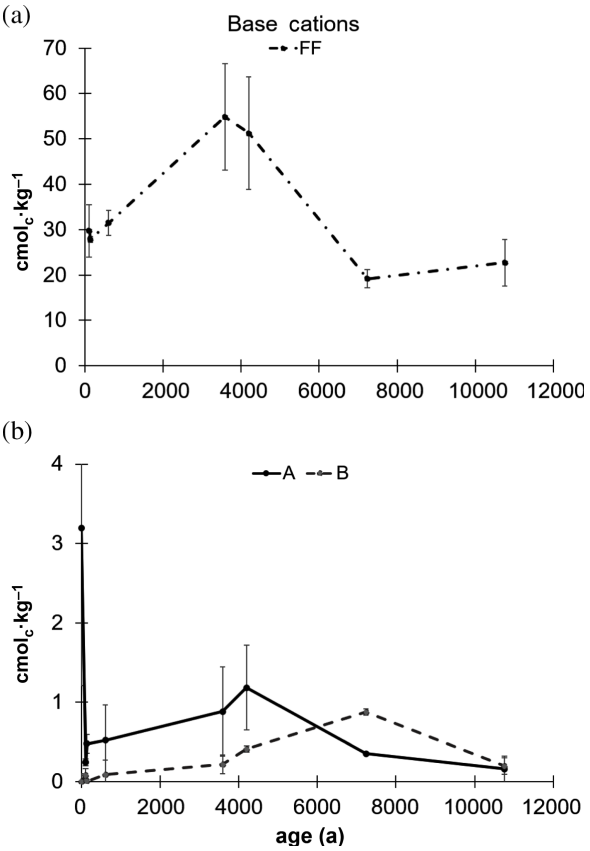

The mass of C to 1 m depth, including the FF, increased with age up to 7200 a and then plateaued, and was fit with a Michaelis–Menton non-linear model (Fig. 4). The highest C mass was present on the 7236 a site (47.3 kg·m^{-2}), and the lowest was on the youngest site (~0 a; 6.3 kg·m^{-2}). Total C mass on the oldest site (10 760 a; 23.9 kg·m^{-2}) was less than on the 7236 a site.

The peaks of Fe_p in the depth profile corresponded to the presence of placic horizons, whereas peaks of Al_p represented either ortstein or placic horizons (Fig. 5). Replicate A on the 3588 a site (CIDS8A) had the greatest Fe_p concentration, followed by the oldest site replicate A (10 760 a) and then replicate B on the 3588 a site (Fig. 5*a*). The CIDS10A pedon had the greatest Al_p concentration, followed by CIDS8B, CIDS8A, and CIDS10B (Fig. 5*b*).

The concentrations of amorphous Fe (Fe_o-Fe_p) and Al (Al_o-Al_p) increased with increasing age (Figs. 5*c*, 5*d*). Peaks in amorphous Fe did not always correspond to peaks in Fe_p, and the concentration of Fe_o-Fe_p decreased with increasing depth (Figs. 5*a*, 5*c*). Pyrophosphate-extractable Fe concentration ranged from 0.0 g·kg^{-1} in the youngest sites to 19.7 g·kg^{-1} in a

Fig. 4. Average mass of carbon (C) to 1 m depth for each site including the forest floor with one standard deviation ($n = 2$).

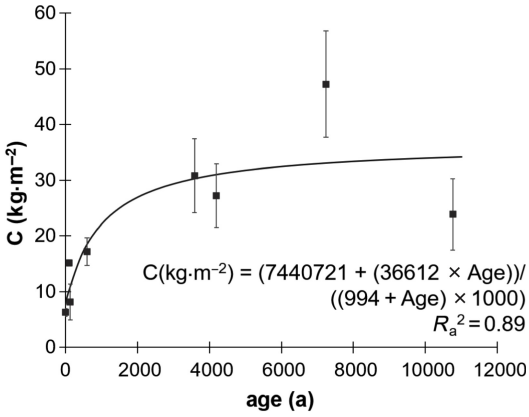

Bfc1 (3588 a). Oxalate-extractable Fe ranged from 0.0 g·kg^{-1} in an Ahb (0 a) to 34.2 g·kg^{-1} in a Bfc2 (3588 a; Supplementary Table S3[1]). The total Fe concentration (Fe_T) in all horizons and ages ranged from 2.03 g·kg^{-1} in an Ae horizon (4198 a) to 43.2 g·kg^{-1} in a Bfc2 (3588 a; Supplementary Table S3[1]). The total amorphous Al concentration increased with increasing age. Amorphous Al was distributed throughout the profile for both replicates on the 3588 a site compared with the youngest site (~0 a; Fig. 5*d*). Replicate B on the oldest site (10 760 a; CIDS10B) had an apparent peak of amorphous Al where the Bfc and Bmcj horizons were present, whereas the concentration of amorphous inorganic Al was relatively consistent with depth on site CIDS10A (Fig. 5*d*). The proportion of total Fe that was oxalate extractable was much greater than for Al (Nelson 2018). There was no clear separation with depth of pyrophosphate- or oxalate-extractable Fe and Al; however, appreciable concentrations of extractable Al (>1.0 g·kg^{-1}) extended to depths greater than extractable Fe (Supplementary Table S3[1]).

Estimated allophanic materials increased in abundance with increasing age (Fig. 6*a*; Supplementary Table S3[1]) with the B horizons on sites less than 3600 a exhibiting estimated allophane concentrations of 0.0–5.0 g·kg^{-1}, whereas sites >3600 a had estimated allophane concentrations of 0.0–41 g·kg^{-1}. Interestingly, the highest estimated allophane concentrations were not correlated to the greatest percent clay, although horizons with >5.0 g·kg^{-1} estimated allophane typically had more clay than those without allophane. The youngest site, ~0 a (CIDS1A), had a consistent, but minimal, concentration of estimated allophane throughout the entire profile. Soil depth profiles indicated increasing concentrations of allophane with increasing age, particularly in Ae, Bhc, and Bfc horizons (Fig. 6*a*). The peaks of estimated allophane concentration occurred closer to the surface in the older soils with estimated allophane

Fig. 5. (*a*) Pyrophosphate-extractable iron (Fe_p), (*b*) pyrophosphate-extractable aluminum (Al_p), (*c*) amorphous inorganic Fe [oxalate-extractable Fe (Fe_o) — Fe_p], and (*d*) amorphous inorganic Al [oxalate-extractable Al (Al_o) — Al_p] in selected pedons to 90 cm depth: 0 yr before present (a; site CIDS1, replicate A), 3588 a (site CIDS8, replicates A and B), 10 760 a (site CIDS10, replicates A and B).

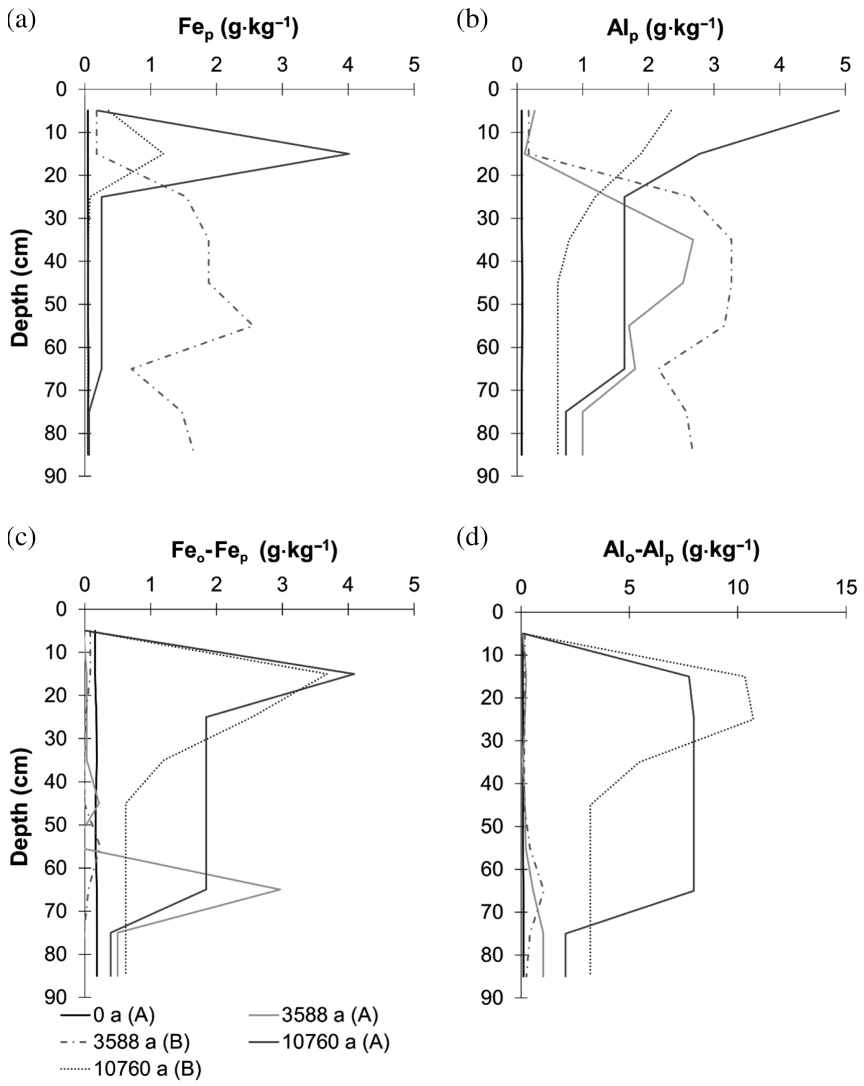

concentrations >35 g·kg^{-1} in the Bfc horizons at 10–15 cm depth on the 10 760 a site (both replicates), whereas the peak concentrations (>3.0 %) of estimated allophane on the 3588 a site was at depths greater than 57 cm in the Bfc2 (replicate A) and Bfcj1 horizons (replicate B) (Fig. 6*a*; Supplementary Table S3[1]). The 4198 a site (CIDS15) had the greatest concentration of allophane compared with all other soil profiles (Supplementary Table S3[1]).

The average CIA for the assumed parent geological material was 44.5 ($n = 2$; Fig. 6*b*). All pedons had CIA values greater than the assumed parent geological material, except for the Ahb2 horizon on the youngest site (replicate A) that had a CIA value of 42.8 (Supplementary Table S3[1]), and with increasing age, the CIA ratio for all soil profiles increased. The 3588 a site had similar CIA values for both soil profiles, reaching a plateau around 49 in the B horizons (Fig. 6*b*). The CIA depth profiles for the oldest site (10 760 a) replicates followed similar trends, with the greatest CIA in the Bfc and Bmcj horizons. The highest CIA value identified on the chronosequence was in the Bfc horizons on the 10 760 a site with a CIA value of 55.2 (Fig. 6*b*; Supplementary Table S3[1]).

Aboveground biomass

Basal area was variable within and among sites (Fig. 7). The youngest site did not have any trees over 1.3 m height. With increasing landform age, the average BA increased until 3588 ± 303 a followed by a decline, except for the 605 a site (Fig. 7). The 605 a site did not have a consistent successional stage throughout due to significant tree fall. Only one of the three BA plots was in a mature forest so there was high variability within the 605 a site BA data (see Nelson 2018). Representative photographs

Fig. 6. Selected soil depth profiles for (*a*) estimated allophane (%) and (*b*) chemical index of alteration (CIA) values in the <2 mm fraction, with reference values for the assumed parent geological material determined for the deepest identified C horizons at the youngest site (site CIDS1; $n = 2$): 0 yr before present (a; site CIDS1, replicate A), 3588 a (site CIDS8, replicates A and B), 10 760 a (site CIDS10, replicates A and B). [Colour online.]

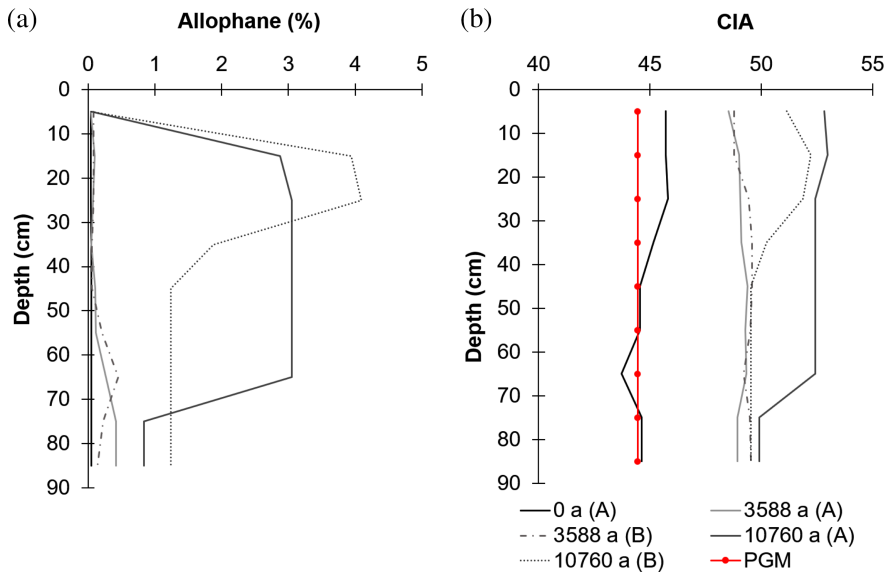

Fig. 7. Tree basal area (BA) on each site by age [years before present (a); $n = 3$]. Standard deviation is indicated by error bars.

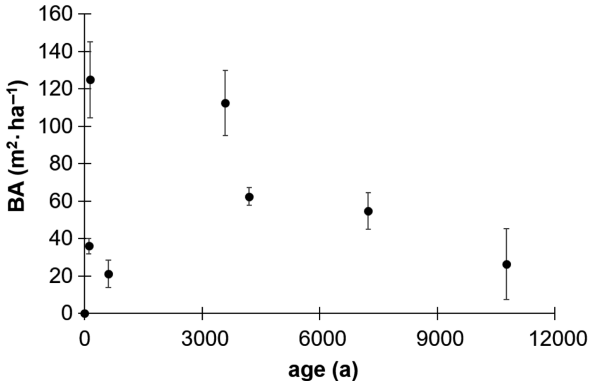

Fig. 8. Characteristic photographs of the three successional stages present on the Calvert Island chronosequence; the progressive (build-up) phase (~0 a; CIDS1), maximal biomass phase (3588 a; CIDS8), and the retrogressive (decline) phase (10 760 a; CIDS10). [Colour online.]

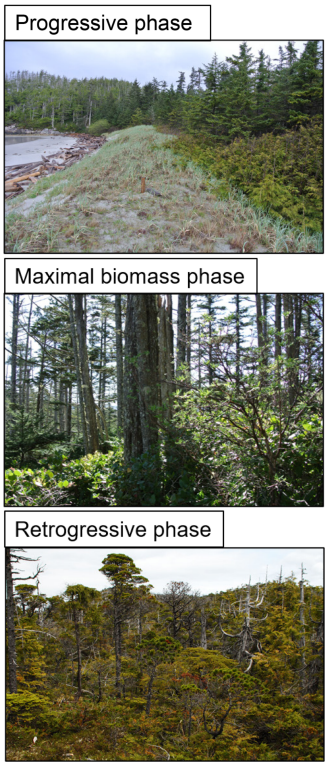

of the youngest site, ~0 a, an intermediate site, 3588 a, and the oldest site, 10 760 a (Fig. 8), display the build-up phase, maximal biomass phase, and decline phase, respectively, illustrating the decline in aboveground biomass with increasing age.

The youngest site had an early seral stage plant community consisting mostly of dune wildrye grass [*Leymus mollis* (Trin.) Pilg. subsp. *mollis*] and red fescue (*Festuca rubra* L. subsp. *rubra*) with other species that grow easily on naturally disturbed coastal dunes including yarrow (*Achillea millefolium* L.), Indian paintbrush (*Castilleja miniata* Dougl. Ex. Hook. var. *miniata*),

Table 2. Nitrogen (N) and phosphorus (P) concentrations and ratio in western redcedar and western hemlock foliage with the standard deviation in brackets if applicable (otherwise the replicate of the sample is denoted), Calvert Island chronosequence.

Species	Site age (a)/replicate	N ($g \cdot kg^{-1}$)	P ($g \cdot kg^{-1}$)	N:P[a]
Western redcedar	139 ± 17 (replicate A)	9.7	1.4	6.9
	605 ± 50 (replicate B)	7.5	1.0	7.5
	4198 ± 332	7.6 (0.2)	0.8 (0.0)	9.5
	7236 ± 546 (replicate B)	5.5	0.6	9.2
	10 760 ± 864 (replicate B)	4.5	0.4	11.3
Western hemlock	105 ± 15	8.0 (1.2)	1.2 (0.2)	6.7
	139 ± 17	8.0 (0.3)	1.3 (0.0)	6.2
	605 ± 50 (replicate A)	6.7	1.8	3.7
	3588 ± 303	7.3 (1.2)	1.1 (0.2)	6.6
	4198 ± 332	6.2 (0.6)	0.8 (0.0)	7.8
	7236 ± 546	5.5 (0.3)	0.5 (0.0)	11.0
	10 760 ± 864	5.1 (0.5)	0.5 (0.0)	10.2

[a]Mass basis.

coastal strawberry, and peavine (*Lathyrus japonicus* Willd.; Supplementary Table S4[1]). Red alder was only present on the 105 and 605 a sites. Sitka spruce was present on most intermediate-aged sites from 105 ± 15 to 4198 ± 332 a (Supplementary Table S4[1]). After 7236 ± 546 a, yellow cedar, mountain hemlock [*Tsuga mertensiana* (Bong.) Carr.], and shore pine became more dominant tree species and were associated with an increase in sphagnum moss (*Sphagnum* sp.) and Labrador tea (*Rhododendron groendlandicum* Oeder; Supplementary Table S4[1]).

Foliar N and P

Nitrogen concentrations declined from 9.7 $g \cdot kg^{-1}$ at the 139 a site to 4.5 $g \cdot kg^{-1}$ at the oldest site in western redcedar, and from 8.0 $g \cdot kg^{-1}$ (SD 1.2) to 5.1 $g \cdot kg^{-1}$ (SD 0.5) in western hemlock (Table 2). Phosphorus concentrations declined to a greater extent over the chronosequence, from 1.4 $g \cdot kg^{-1}$ at 139 ± 17 a to 0.4 $g \cdot kg^{-1}$ at 10 760 ± 864 a in western redcedar (Table 2). For western hemlock, the peak P concentration of 1.8 $g \cdot kg^{-1}$ occurred at 605 a, declining to 0.5 $g \cdot kg^{-1}$ (SD 0.0) on the 10 760 a site. As a result of these trends, the foliar N:P ratios gradually increased over time, reaching a maximum of 11.3 at the oldest site, and 10.2 at the second oldest site, for western redcedar and western hemlock, respectively (Table 2).

Discussion

Soil development trends and processes

Within the first 100 yr of soil development in this hypermaritime chronosequence, the soil morphological changes suggest that podzolization was the dominant soil-forming process. This rapid development can be attributed to the temperate climate and high rainfall (approximately 2800 $mm \cdot a^{-1}$; Supplementary Table S1[1]). It took <105 ± 15 a of pedogenesis to develop a distinct eluvial horizon beneath a FF with well-differentiated S/L, F, and H horizons. Between 139 ± 17 and 605 ± 50 a, the development of an organic-enriched, weakly cemented B horizon occurred. By 3588 ± 303 a, a mature Podzol formed with both ortstein and placic horizons.

The primary cementing agents in placic horizons were organically complexed Fe and Al, whereas ortsteins were cemented by organically complexed Al and organic material. Some developing ortsteins, such as Bmcj horizons, were less enriched in organic material, but organically complexed Al was the likely cementing agent, consistent with findings by McKeague and Wang (1980), Lapen and Wang (1999), and Sanborn et al. (2011).

The base cation concentration in the FF was significantly higher than in the mineral soil, most likely due to surface enrichment from litter fall and the close proximity to sea spray. All sites were within approximately 310 m from the shoreline, with the 3588 and 4198 a sites being closest (140 m). On the west coast of Vancouver Island, sea spray can deposit on the order of 250 $g \cdot m^{-2}$ of Na, 22 $g \cdot m^{-2}$ of Mg, 8.9 $g \cdot m^{-2}$ of K, and 7.0 $g \cdot m^{-2}$ of Ca annually (Cordes 1972; Sondheim et al. 1981). The peak base cation concentration within the FF on the 3588 and 4198 a sites may be attributed to litterfall from the dominant yellow and redcedar, which are known to have high Ca concentrations (Radwan and Harrington 1986). However, the mineral horizons had continual depletion of base cations with age.

Chemical index of alteration

Granite and granodiorite are the prevalent bedrock types on northern Calvert Island and may be the main source of these sandy parent geological material, given the thin, discontinuous cover of glacial deposits (Roddick 1996; Neudorf et al. 2015). Generally, CIA values for granite and granodiorite are between 45 and 55 (Nesbitt and Young 1982), which brackets the range

Fig. 9. Conceptual depiction of soil and forest development with increasing age along the Calvert Island chronosequence including the development of cemented ortstein (Bhc) and placic (Bfc) horizons with age and the dominance of stunted tree growth on the oldest sites. Note that implied horizon thicknesses in this diagram are relative, not absolute. For reference, the actual elevation range across the chronosequence is 3.6–34.6 m above sea level. Tree icons adapted from Banner et al. (1993) with permission [Copyright © Province of British Columbia. All rights reserved. Reproduced with permission of the Province of British Columbia].

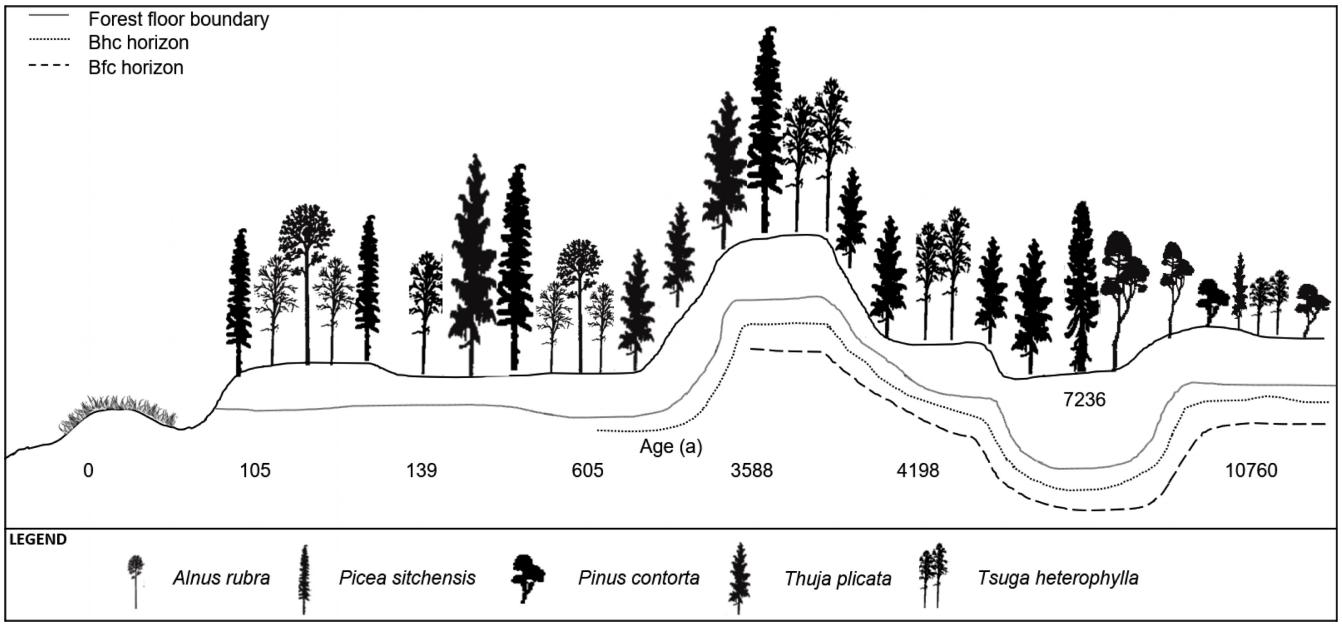

calculated from geochemical data for bedrock samples from Calvert and Hecate Islands (Roddick 1996; G. Woodsworth, personal communication). The limited change in CIA over the Calvert Island chronosequence with increasing age was unexpected, considering that (*i*) these soils were classified as mature Podzols after 3588 a, (*ii*) they exhibit strong morphological development, and (*iii*) they have formed in a wet, mild climate highly conducive to chemical weathering and leaching. The weathering regime experienced by these soils may be severe enough that it approaches congruent dissolution of the primary minerals, with limited formation of secondary phases, as suggested by low concentrations of clay (<~9.1%) and amorphous materials (<~41 $g{\cdot}kg^{-1}$ allophane).

Mechanisms of podzolization

Iron concentrations in bedrock in the study area were inherently low compared with values determined along a ~200 km transect extending eastward from Calvert Island, spanning the Coast Range (Roddick 1996; G. Woodsworth, personal communication). The average total Fe values for the transect were 40 $g{\cdot}kg^{-1}$ (SD = 20), whereas the average Fe values for sampling locations on Calvert and Hectate Islands were 16 $g{\cdot}kg^{-1}$ (SD = 17; Roddick 1996; G. Woodsworth, personal communication). As noted above, local bedrock is likely a major source of glacial sediment that was reworked into the sand forming the dunes of this chronosequence. Soils with low Fe concentrations (particularly below 50 $g{\cdot}kg^{-1}$) promote podzolization over brunification, and the development of Mor and Moder humus forms rather than Mull forms (Douchaufour and Souchier 1978). Low-Fe parent materials are often also low in clay and are often acidic, which causes a lower OM decomposition rate compared with parent materials high in Fe and clay (Douchaufour and Souchier 1978). The soils of the Calvert Island chronosequence were dominated by Mor and Moder humus forms, had low total Fe concentrations (<39 $g{\cdot}kg^{-1}$) in uncemented horizons, low clay (<9.1 %) concentrations, and the dominance of organic-enriched Bh horizons rather than Bhf or Bf horizons; this suggests that the low-Fe parent material influenced the path of pedogenesis for this sequence of soils. Organically complexed Al and Fe were present after 605 ± 50 a within humic-enriched horizons, whereas estimated allophane did not achieve appreciable concentrations (>5.0 $g{\cdot}kg^{-1}$) until after 3600 a. This suggests that the podzolization mechanism of organo-metallic complexation must have occurred prior to the formation of allophane. Cemented horizons formed between 139 ± 17 and 605 ± 50 a of soil development and may have acted as a barrier, impeding the movement of organic or inorganic sols. Therefore, the Al in the allophanic materials may have been derived from organo-metal complexes that were deposited prior to formation of water-restricting features and could have been enhanced by the upward movement of Al derived from parent

material with ground water fluxes (Dahlgren and Ugolini 1989; Ugolini and Dahlgren 1991).

Comparison of soil development rates

Local comparisons

Podzolization rates on Calvert Island were most comparable to the Naikoon chronosequence located approximately 360 km to the northwest on the Haida Gwaii archipelago (Fig. 1*a*), where it took <3100 a to form a Placic Humic Podzol (Sanborn and Massicotte 2010). On western Vancouver Island at Cox Bay (approximately 320 km to the southeast of Calvert Island; Fig. 1*a*), it took ~371 a to form a mature Podzol, likely owing to the slightly wetter and warmer climate (Singleton and Lavkulich 1987*a*). Soils at Cox Bay lacked placic horizons, presumably due either to their youthfulness or to parent material chemistry. Formation of placic horizons took between 1200 and 5000 a on the Brooks Peninsula chronosequence and between 800 and 3100 a on the Naikoon chronosequence (Maxwell 1997; Sanborn and Massicotte 2010) compared with 605 ± 50 to 3588 ± 303 a on Calvert Island. Similar to the Naikoon chronosequence, placic horizons on Calvert Island were not enriched in Mn as was observed in Newfoundland (McKeague et al. 1968; Moore 1976; Sanborn and Massicotte 2010).

The time required for formation of Podzols and cemented horizons in Canada is highly variable because of the wide range of climates, parent materials, plant community compositions (and litter inputs), and duration of pedogenesis. For instance, Podzol formation was identified on the Hudson Bay chronosequence after 2300 a and after ~1200 a in southern James Bay (Protz et al. 1984, 1988). Within soils near the St. Lawrence River, Quebec, where the mean annual precipitation (MAP) is roughly one-third that on Calvert Island, it took 5000–6000 a to form a placic horizon (Moore 1976). Dubois et al. (1990) documented locations in Quebec where ortstein development occurred in less than 420 a, which was similar to their rate of formation inferred from the Calvert Island chronosequence. Similar to Calvert Island, ortsteins on the east coast of Canada (New Brunswick, Nova Scotia, and southern Newfoundland) are primarily cemented by organic-Al complexes (McKeague and Wang 1980; Lapen and Wang 1999).

It is important to note that comparing rates of podzolization in soils outside Canada can be difficult due to differences in analytical methods and classification criteria to define Podzols. However, comparisons with other sites within the North American coastal temperate rainforest are particularly useful for the Calvert Island chronosequence. In southeast Alaska, Podzols formed within 300 a or less at the Mendenhall glacier chronosequence with >2500 mm of MAP, with characteristic Bf and C horizons apparent after 100 a (Alexander and Burt 1996). Within 6000–8000 a in Lituya Bay, Alaska, Podzolic soil horizons developed with the rapid (i.e., within 500 a) formation of placic horizons followed by paludification and the reduction/removal of Fe from the soil profile (Ugolini and Mann 1979). These results demonstrate that podzolization rates in southeast Alaska, approximately 390 km northwest of Calvert Island, are comparable.

Global comparisons

When MAP and mean annual temperature (MAT) are taken into consideration, the podzolization rates on Calvert Island can also be compared with sites outside North America. In the northern hemisphere, reported rates of Podzol formation range from 1000 a in a subarctic climate in northern Sweden (Jenny 1941) to 6600 a in Norway in an area with a lower MAT and significantly less MAP (Sauer et al. 2007). In the southern hemisphere, the Cooloola chronosequence in Australia developed a mature Podzol within 7500 a with proto-imogolite allophanic materials in the Bhs and Bh horizons, similar to Calvert Island (Skjemstad et al. 1992).

The Haast chronosequence in New Zealand is an example of rapid Podzol development in a climate both warmer and wetter than the Calvert Island chronosequence (Eger et al. 2011; Turner et al. 2012). This series of soils was also formed on foredune ridges and has a uniform parent material of quartzo-feldspathic sand (Eger et al. 2011). Within 3903 a, the dunes met the criteria for a Spodosol (the USA classification most similar to Podzol) and had developed placic horizons between 370 and 1000 a (Eger et al. 2011; Turner et al. 2012). As such, the Haast chronosequence is perhaps the most comparable chronosequence globally to Calvert Island due to similar parent geological material, and rates of podzolization.

Long-term ecosystem development

Plant communities on the Calvert Island chronosequence appear to have shifted from early successional plant communities on the youngest site (~0 a) to climax plant communities on intermediate-aged sites (3588 and 4198 a), followed by a less-productive plant community that was adapted to poorer and wetter soil conditions by 10 760 ± 864 a (Figs. 8 and 9) (Banner et al. 2005). The younger and intermediate-aged sites on Calvert Island had more productive forest types CWHvh2 – 01 CwHw Salal (zonal forest) and 15-Ss Kindbergia (higher productivity, shoreline forest), whereas the older sites were 11-CwYc goldthread (bog forest), which are classified as low-productivity forests (Kranabetter et al. 2005). The distribution of tree BA along the Calvert Island chronosequence increased to a maximum followed by a decline as expected for a retrogressed chronosequence, despite the significant tree throw on the 605 a site. Tree throws occur frequently on Calvert Island due to high exposure to strong winter storm winds and because trees are typically shallowly

rooted. As a result, trees on Calvert Island rarely live longer than 300 a.

The mass of total C on the 10 760 a site was less than the mass on the 7236 a site, partly due to differences in site microtopography, drainage, slope position, and resultant FF development, which resulted in the younger site accumulating a FF horizon thick enough to be classified as organic soil. Therefore, the mass of total C on the 7236 a site was uncharacteristically high. If this site were located in a comparable upland landscape position, it is likely that the mass of total C would follow the expected trend of increasing to a maximum and plateauing with increasing age; as such, the data were analyzed with a Michaelis–Menton non-linear model (Wardle et al. 2004; Wardle et al. 2008; Peltzer et al. 2010).

We previously reported significant declines in total P reserves along the Calvert Island chronosequence with increasing age and a shift towards more recalcitrant forms of organic P, consistent with the Walker and Syers (1976) model of long-term soil P dynamics (Nelson et al. 2020). Despite these trends, evidence for P limitation to tree growth in the later phases of the chronosequence is mixed. Although N:P ratios in tree foliage generally increased over time in this study, the values are not extreme in relation to the ranges observed elsewhere for other types of forest vegetation (Güsewell 2004). However, it is apparent that ecosystem retrogression is occurring on the older sites of the Calvert Island chronosequence, which may be caused by some combination of reduced P supply and soil physical changes, such as impedance of root penetration and water movement resulting from cemented horizons forming within the rooting zone.

Retrogression is most frequently associated with a depletion-driven system where P within the soil has been utilized and lost with increasing age, causing a reduction in primary productivity as illustrated by the Walker and Syers (1976) model (Wardle et al. 2004). Vitousek et al. (2010) further explained mechanisms that may influence the path of retrogression, such as soil barriers, low P parent material, transactional limitations due to difficulties releasing P from parent material, and anthropogenic causes. Two retrogressive chronosequences, Waitutu, NZ and Glacier Bay, Alaska, had severe alterations to soil drainage associated with a shift in plant communities as well as P limitations (Wardle et al. 2004). Gaxiola et al. (2010) found higher water table height to be significantly correlated to BA declines on Waitutu. The Mendocino, California, chronosequence is another well-known case study where iron pans, formed on older sites, may contribute to ecosystem retrogression (Jenny et al. 1969). The Haast chronosequence had placic horizon formation in <4000 a, which is thought to have ecological significance as a driver of retrogression (Turner et al. 2012).

The Glacier Bay chronosequence is very similar to the Calvert Island chronosequence because they are both within the coastal temperate rainforest and both exhibit retrogression after ~11 000 a (Wardle et al. 2004). Similar plant communities exist at the Calvert Island chronosequence after 7236 ± 546 a and the Glacier Bay chronosequence after 11 000 a, with dominant species including crowberry (*Empetrum nigrum* L.), Labrador tea, sphagnum moss, mountain hemlock, and shore pine (Wardle et al. 2004). Noble et al. (1984) concluded that podzolization raised the water table in Glacier Bay, which was further accelerated by the presence of sphagnum moss.

The Calvert Island chronosequence documents the long-term trends in BA and changes in plant communities that accompany ageing aeolian soils on the coast of BC. This information is useful for understanding the potential mechanisms of reduced tree growth in low-productivity forests on the coast. The knowledge gained from this study can be used to further inform the mechanisms of ecosystem and soil development on the Cox Bay and Naikoon chronosequences. Lastly, this study can be added to the global repository of documented chronosequences experiencing retrogression, to further the understanding of this concept.

Conclusions

Soil development in the Calvert Island chronosequence has been facilitated by its hypermaritime environment and coarse-textured parent material. After approximately 605 ± 50 a, an FF, eluvial horizon, and weakly cemented B horizons had formed. Within 3500 a, a mature Podzol had developed with characteristic placic and ortstein horizons. The rate of soil development was comparable to the Cox Bay and Naikoon chronosequences in BC and the Haast chronosequence in New Zealand. Base cation concentrations remained relatively consistent with age in the FF but declined considerably in the A and B horizons. Amorphous Fe and Al concentrations increased with increasing age, whereas maximum concentrations of organically complexed Fe and Al occurred in cemented placic and ortstein horizons. Formation and transport of organo-metallic complexes appeared to be the dominant mechanism involved in podzolization. Despite an environment highly conducive to weathering, all soils had relatively low values of a common weathering index (CIA), suggesting that congruent dissolution may be occurring.

Ecosystem retrogression is apparent in the latter stages of the Calvert Island chronosequence — a phenomenon not previously documented in coastal BC. This information furthers our understanding of the connections between soil development, nutrient status, and site productivity in the temperate rainforests of coastal BC. The hump-shaped curve in BA and a shift with age towards tree species more tolerant of the declining soil fertility were apparent. Consistent with other retrogressive chronosequence, the mass of total C with age increased to a plateau, illustrating the accumulation of C with ecosystem development. Further research is

needed to determine the relative contributions of nutrient (especially P) limitation, soil physical barriers, and other possible drivers of this pattern of long-term ecosystem development to ecosystem retrogression on the Calvert Island chronosequence.

Competing Interests

The authors declare there are no competing interests.

Author Contributions

L.-A.N. wrote the bulk of the manuscript, with all co-authors contributing to editing and revision. P.S. and B.C.-M. supervised field work and data analysis. I.W., O.L., and P.S. conducted the initial field work which selected the study area and identified its suitability for this study.

Funding

Financial and logistical support were provided by the Hakai Institute to I.W., P.S., and O.L. as part of its Coastal Sandy Ecosystems Program. O.L. acknowledges support from the Natural Sciences and Engineering Research Council of Canada Discovery Grant and Research Tools and Instruments Grant programs.

Data Availability Statement

Data are available on request to the corresponding author.

Acknowledgements

We recognize and are grateful for the opportunity to complete this study on the traditional territory of the Heiltsuk and Wuikinuxv First Nations. We would particularly like to thank Lori Johnson for her hard work in the field. We thank Christina Neudorf for her work in obtaining the OSL ages which made this study possible, and for allowing us to adapt her study area map. Nancy Alexander produced the regional location map. Lastly, we would like to thank Glenn Woodsworth for sharing unpublished Geological Survey of Canada bedrock geochemistry data.

References

Alexander, E.B., and Burt, R. 1996. Soil development on moraines of Mendenhall Glacier, southeast Alaska. I. The moraines and soil morphology. Geoderma, **72**: 1–17. doi:10.1016/0016-7061(96)00021-3.

Ballard, T.M., and Carter, R.E. 1986. Evaluating forest stand nutrient status (LMH No. 20). Information Services Branch Ministry of Forests, Victoria, BC, Canada. 70 pp.

Banner, A., Mackenzie, W., Haeussler, S., Thomson, S., Pojar, J., and Trowbridge, R. 1993. A field guide to site identification and interpretation for the Prince Rupert forest region (LMH No. 26). Information Services Branch Ministry of Forests, Victoria, BC, Canada. 281 pp.

Banner, A., LePage, P., Moran, J., and de Groot, A. 2005. The HyP3 Project: pattern, process, and productivity in hypermaritime forests of coastal British Columbia — a synthesis of 7-year results (Spec. Rep. 10). British Columbia Ministry of Forest, Research Branch, Victoria, BC, Canada. 161 pp.

Blake, H.R., and Hartge, K.H. 1986. Bulk density. Pages 363–375 in A. Klute, ed. Methods of soil analysis. Part 1. Agronomy. American Society of Agronomy, Madison, WI, USA.

Claisse Inc. 2003. Glass disks and solutions by fusion for Claisse Fluxer users manual. Claisse Inc. 67 pp.

Coomes, D.A., Allen, R.B., Bentley, W.A., Burrows, L.E., Canham, C.D., Fagan, L., et al. 2005. The hare, the tortoise and the crocodile: the ecology of angiosperm dominance, conifer persistence and fern filtering. J. Ecol. **93**: 918–935. doi:10.1111/j.1365-2745.2005.01012.x.

Cordes, L.D. 1972. An ecological study of the Sitka spruce forest on the west coast of Vancouver Island. Ph.D. thesis, The University of British Columbia, Vancouver, BC, Canada. 467 pp.

Courchesne, F., and Turmel, M.-C. 2008. Extractable Al, Fe, Mn, and Si. Pages 307–312 in M.R. Carter and E.G. Gregorich, eds. Soil sampling and methods of analysis. Taylor & Francis Group, Boca Raton, FL, USA.

D'Amore, D.V., Ping, C.-L., and Herendeen, P.A. 2015. Hydromorphic soil development in the coastal temperate rainforest of Alaska. Soil Sci. Soc. Am. J. **79**: 698–709. doi:10.2136/sssaj2014.08.0322.

Darvill, C.M., Menounos, B., Goehring, B.M., Lian, O.B., and Caffee, M.C. 2018. Deglaciation of the western Cordilleran Ice Sheet. Geophys. Res. Lett. **45**: 9710–9720. doi:10.1029/2018GL079419.

Dahlgren, R.A., and Ugolini, F.C. 1989. Formation and stability of imogolite in a tephritic Spodosol, Cascade Range, Washington, USA. Geochim. Cosmochim. Acta, **53**: 1897–1904. doi:10.1016/0016-7037(89)90311-6.

Duchaufour, P., and Souchier, B. 1978. Roles of iron and clay in genesis of acid soils under a humid, temperate climate. Geoderma, **20**: 15–26. doi:10.1016/0016-7061(78)90046-0.

Dubois, J.-M., Martel, Y.A., and Nadeau, L. 1990. Les ortsteins du Québec: répartition geographique, relations géomorphologiques et essai de datation. Can. Geogr. **34**: 303–317. doi:10.1111/j.1541-0064.1990.tb01269.x.

Eamer, J.B.R. 2017. Reconstruction of the late Pleistocene and Holocene geomorphology of northwest Calvert Island, British Columbia. Ph.D. thesis, University of Victoria, Victoria, BC, Canada. 133 pp.

Eamer, J.B.R., Shugar, D.H., Walker, I.J., Lian, O.B., Neudorf, C.M., and Telka, A.M. 2017. A glacial readvance during retreat of the Cordilleran Ice Sheet, British Columbia central coast. Quat. Res. **87**: 468–481. doi:10.1017/qua.2017.16.

Eamer, J.B.R., Shugar, D.H., Walker, I.J., Neudorf, C.M., Lian, O.B., Eamer, J.L., et al. 2018. Late Quaternary landscape evolution in a region of stable postglacial relative sea levels, British Columbia central coast, Canada. Boreas, **47**: 738–753. doi:10.1111/bor.12297.

Eger, A., Almond, P.C., and Condron, L.M. 2011. Pedogenesis, soil mass balance, phosphorus dynamics and vegetation communities across a Holocene soil chronosequence in a superhumid climate, south Westland, New Zealand. Geoderma, **163**: 185–196. doi:10.1016/j.geoderma.2011.04.007.

Farmer, V., and Fraser, A.R. 1982. Chemical and colloidal stability of sols in the Al_2O_3-Fe_2O_3-SiO_2-H_2O system: their role in podzolization. J. Soil. Sci. **33**: 737–742. doi:10.1111/j.1365-2389.1982.tb01803.x.

Gaxiola, A., McNeill, S.M., and Coomes, D. 2010. What drives retrogressive succession? Plant strategies to tolerate infertile and poorly drained soils. Funct. Ecol. **24**: 714–722. doi:10.1111/j.1365-2435.2010.01688.x.

Gee, G.W., and Bauder, J.W. 1986. Particle-size analysis. Pages 331–362 in A. Klute, ed. Methods of soil analysis. Part I. Physical and mineralogical methods. Agronomy Monograph. Vol. 9. Soil Science Society of America, Madison, WI, USA.

Güsewell, S. 2004. N:P ratios in terrestrial plants: variation and functional significance. New Phytol. **164**: 243–266. doi:10.1111/j.1469-8137.2004.01192.x. PMID:33873556.

Gustafsson, J.P., Bhattacharya, P., Bain, D.C., Fraser, A.R., and McHardy, W.J. 1995. Podzolisation mechanisms and the synthesis of imogolite in northern Scandinavia. Geoderma, **66**: 167–184. doi:10.1016/0016-7061(95)00005-9.

Hebda, R.J. 1995. British Columbia vegetation and climate history with focus on 6 ka. Geogr. Phys. Quat. **49**: 55–79.

Hoffman, K., Gavin, D., Lertzman, K., Smith, D., and Starzomski, B. 2016. 13,000 years of fire history derived from soil charcoal in a British Columbia coastal temperate rainforest. Ecosphere, **7**: 1–13. doi:10.1002/ecs2.1415.

Jenny, H. 1941. Factors of soil formation: a system of quantitative pedology. McGraw-Hill, New York, NY, USA. 281 pp.

Jenny, H., Arkley, R.J., and Schultz, A. 1969. The pygmy forest-Podsol ecosystem and its dune associates of the Mendocino coast. Madroño, **20**: 60–74.

Kranabetter, J.M., Banner, A., and de Groot, A. 2005. An assessment of phosphorus limitations to soil nitrogen availability across forest ecosystems of north coastal British Columbia. Can. J. For. Res. **35**: 530–540. doi:10.1139/x04-192.

Lafortune, V., Filion, L., and Hétu, B. 2006. Émersion des terres et développement des sols bien drainés au Lac Guillaume-Delisle, Québec subarctique. Geogr. Phys. Quat. **60**: 165–181. doi:10.7202/016827ar.

Lapen, D.R., and Wang, C. 1999. Placic and ortstein horizon genesis and peatland development, Southeastern Newfoundland. Soil Sci. Soc. Am. J. **63**: 1472–1482. doi:10.2136/sssaj1999.6351472x.

Mathewes, R., and Clague, J. 2017. Paleoecology and ice limits of the early Fraser glaciation (Marine Isotope Stage 2) on Haida Gwaii, British Columbia, Canada. Quat. Res. **88**: 277–292. doi:10.1017/qua.2017.36.

Maxwell, R.E. 1997. Soils of Brooks Peninsula. Pages 4.1–4.49 in R.J. Hedba, and J.C. Haggarty, eds. Brooks Peninsula: an ice age refugium on Vancouver Island (Occasional Paper No. 5.). B.C. Min. Environ., Lands and Parks, Victoria, BC, USA.

McKeague, J., and Day, J. 1966. Dithionite-and oxalate-extractable Fe and Al as aids in differentiating various classes of soils. Can. J. Soil Sci. **46**: 13–22. doi:10.4141/cjss66-003.

McKeague, J., and Wang, C. 1980. Micromorphology and energy dispersive analysis of ortstein horizons of Podzolic soils from New Brunswick and Nova Scotia, Canada. Can. J. Soil Sci. **60**: 9–21. doi:10.4141/cjss80-002.

McKeague, J., Damman, A., and Heringa, P. 1968. Iron-manganese and other pans in some soils of Newfoundland. Can. J. Soil Sci. **48**: 243–253. doi:10.4141/cjss68-034.

McKeague, J., DeConinck, F., and Franzmeier, D. 1983. Spodosols. Dev. Soil Sci. **11**: 217–252.

McLaren, D., Fedje, D., Hay, M.B., Mackie, Q., Walker, I.J., Shugar, D.H., et al. 2014. Post-glacial sea level hinge on the central Pacific coast of Canada. Quat. Sci. Rev. **97**: 148–169. doi:10.1016/j.quascirev.2014.05.023.

Ministry of Environment (MOE). 2016. Ecology: ecoregion unit descriptions. [Online]. Available from http://www.env.gov.bc.ca/ecology/ecoregions/humidtemp.html#coast [5 Feb. 2016].

Ministry of Forests and Range. 2010. Field manual for describing terrestrial ecosystems, 2nd. ed. Land Management Handbook 25. Victoria, BC, Canada. 266 pp.

Moore, T. 1976. Sesquioxide-cemented soil horizons in northern Quebec: their distribution, properties and genesis. Can. J. Soil Sci. **56**: 333–344. doi:10.4141/cjss76-042.

National Forest Inventory (NFI). 2008. Canada's national forest inventory ground sampling guidelines, V. 5. Canadian Forest Service, Victoria, BC, Canada. 271 pp.

Nalder, I.A., and Wein, R.W. 1998. A new forest floor corer for rapid sampling, minimal disturbance and adequate precision. Silva Fenn. **32**: 373–382. doi:10.14214/sf.678.

Nelson, L.-A. 2018. Examination of Long-term soil development and phosphorus dynamics in a hypermaritime chronosequence, Calvert Island, British Columbia, Canada. M.Sc. thesis, Department of Natural Resources and Environmental Studies, The University of Northern British Columbia, Prince George, B.C.

Nelson, L.-A., Cade-Menun, B.J., Walker, I.J., and Sanborn, P. 2020. Soil phosphorus dynamics across a Holocene chronosequence of aeolian sand dunes in a hypermaritime environment on Calvert Island, BC, Canada. Front. For. Glob. Change, **3**(83): 1–24.

Neudorf, C.M., Lian, O.B., Walker, I.J., Shugar, D.H., Eamer, J.B.R., and Griffin, L.C.M. 2015. Toward a luminescence chronology for coastal dune and beach deposits on Calvert Island, British Columbia central coast, Canada. Quat. Geochronol. **30**: 275–281. doi:10.1016/j.quageo.2014.12.004.

Nesbitt, H., and Young, G. 1982. Early proterozoic climates and plate motions inferred from major element chemistry of lutites. Nature, **299**: 715–717. doi:10.1038/299715a0.

Noble, M.G., Lawrence, D.B., and Streveler, G.P. 1984. Sphagnum invasion beneath an evergreen forest canopy in southeastern Alaska. Bryologist, **87**: 119–127. doi:10.2307/3243117.

Parfitt, R. 1990. Allophane in New Zealand — a review. Soil Res. **28**: 343–360. doi:10.1071/SR9900343.

Peltzer, D.A., Wardle, D.A., Allison, V.J., Baisden, W.T., Bardgett, R.D., Chadwick, O.A., et al. 2010. Understanding ecosystem retrogression. Ecol. Monogr. **80**: 509–529. doi:10.1890/09-1552.1.

Protz, R., Martini, I., Ross, G., and Terasmae, J. 1984. Rate of podzolic soil formation near Hudson Bay, Ontario. Can. J. Soil Sci. **64**: 31–49. doi:10.4141/cjss84-004.

Protz, R., Shipitalo, M., Ross, G., and Terasmae, J. 1988. Podzolic soil development in the southern James Bay Lowlands, Ontario. Can. J. Soil Sci. **68**: 287–305. doi:10.4141/cjss88-028.

Radwan, M., and Harrington, C.A. 1986. Foliar chemical concentrations, growth, and site productivity relations in western redcedar. Can. J. For. Res. **16**: 1069–1075. doi:10.1139/x86-185.

Roddick, J.A. 1996. Geology, Rivers Inlet (92M) — Queens Sound Map Areas, British Columbia. Open File 3278. Geological Survey of Canada, Ottawa, ON, Canada. 102 pp.

Sanborn, P. 2016. The imprint of time on Canadian soil landscapes. Quat. Int. **418**: 165–179. doi:10.1016/j.quaint.2015.09.053.

Sanborn, P., and Massicotte, H. 2010. A Holocene coastal soil chronosequence: Naikoon Provincial Park, Graham Island, Haida Gwaii: Progress report. University of Northern British Columbia, Prince George, BC, Canada. 53 pp.

Sanborn, P., Lamontagne, L., and Hendershot, W. 2011. Podzolic soils of Canada: Genesis, distribution, and classification. Can. J. Soil Sci. **91**: 843–880. doi:10.4141/cjss10024.

Sauer, D., Sponagel, H., Sommer, M., Giani, L., Jahn, R., and Stahr, K. 2007. Podzol: soil of the year 2007. A review on its genesis, occurrence, and functions. J. Plant Nutr. Soil Sci. **170**: 581–597. doi:10.1002/jpln.200700135.

Sauer, D., Schülli-Maurer, I., Sperstad, R., Sørensen, R., and Stahr, K. 2008. Podzol development with time in sandy beach deposits in southern Norway. J. Plant Nutr. Soil Sci. **171**: 483–497. doi:10.1002/jpln.200700023.

Schaetzl, R., Barrett, L., and Winkler, J. 1994. Choosing models for soil chronofunctions and fitting them to data. Eur. J. Soil Sci. **45**: 219–232. doi:10.1111/j.1365-2389.1994.tb00503.x.

Shugar, D.H., Walker, I.J., Lian, O.B., Eamer, J.B.R., Neudorf, C., McLaren, D., and Fedje, D. 2014. Post-glacial sea-level change along the Pacific coast of North America. Quat. Sci. Rev. **97**: 170–192. doi:10.1016/j.quascirev.2014.05.022.

Singleton, G.A., and Lavkulich, L.M. 1987*a*. A soil chronosequence on beach sands, Vancouver Island, British Columbia. Can. J. Soil Sci. **67**: 795–810. doi:10.4141/cjss87-077.

Singleton, G.A., and Lavkulich, L.M. 1987*b*. Phosphorus transformations in a soil chronosequence, Vancouver Island, British Columbia. Can. J. Soil Sci. **67**: 787–793. doi:10.4141/cjss87-076.

Skjemstad, J., Waters, A.G., Hanna, J.V., and Oades, J.M. 1992. Genesis of podzols on coastal dunes in Southern Queensland. IV. Nature of the organic fraction as seen by 13C nuclear magnetic resonance spectroscopy. Soil Res. **30**: 667–681. doi:10.1071/SR9920667.

Soil Classification Working Group (SCWG). 1998. The Canadian system of soil classification, 3rd ed. Agriculture and Agri-Food Canada, Ottawa, ON, Canada. 202 pp.

Sondheim, M., Singleton, G., and Lavkulich, L. 1981. Numerical analysis of a chronosequence, including the development of a chronofunction. Soil Sci. Soc. Am. J. **45**: 558–563. doi:10.2136/sssaj1981.03615995004500030025x.

Stafford, J., and Christensen,T. 2014. Permit 2010-216 Site EjTa-1, Hakai Beach Institute, Calvert Island: site alteration permit report. Unpublished archaeology report, 56 pp.

Turner, B.L., Condron, L.M., Wells, A., and Andersen, K.M. 2012. Soil nutrient dynamics during Podzol development under lowland temperate rain forest in New Zealand. Catena, **97**: 50–62. doi:10.1016/j.catena.2012.05.007.

Ugolini, F., and Dahlgren, R. 1991. Weathering environments and occurrence of imogolite/allophane in selected andisols and spodosols. Soil Sci. Soc. Am. J. **55**: 1166–1171. doi:10.2136/sssaj1991.03615995005500040045x.

Ugolini, F.C., and Mann, D.H. 1979. Biopedological origin of peatlands in south east Alaska. Nature, **281**: 366–368. doi:10.1038/281366a0.

Vitousek, P.M., Porder, S., Houlton, B.Z., and Chadwick, O.A. 2010. Terrestrial phosphorus limitation: mechanisms, implications, and nitrogen–phosphorus interactions. Ecol. Appl. **20**: 5–15. doi:10.1890/08-0127.1. PMID:20349827.

Walker, L.R., Wardle, D.A., Bardgett, R.D., and Clarkson, B.D. 2010. The use of chronosequences in studies of ecological succession and soil development. J. Ecol. **98**: 725–736. doi:10.1111/j.1365-2745.2010.01664.x.

Walker, T., and Syers, J.K. 1976. The fate of phosphorus during pedogenesis. Geoderma, **15**: 1–19. doi:10.1016/0016-7061(76)90066-5.

Wardle, D.A., Walker, L.R., and Bardgett, R.D. 2004. Ecosystem properties and forest decline in contrasting long-term chronosequences. Science, **305**: 509–513. doi:10.1126/science.1098778. PMID:15205475.

Wardle, D.A., Bardgett, R.D., Walker, L.R., Peltzer, D.A., and Lagerström, A. 2008. The response of plant diversity to ecosystem retrogression: evidence from contrasting long-term chronosequences. Oikos, **117**: 93–103. doi:10.1111/j.2007.0030-1299.16130.x.

Westman, W.E., and Whittaker, R.H. 1975. The pygmy forest region of northern California: Studies on biomass and primary productivity. J. Ecol. **63**: 493–520. doi:10.2307/2258732.

Wolfe, S.A., Walker, I.J., and Huntley, D.J. 2008. Holocene coastal reconstruction, Naikoon peninsula, Queen Charlotte Islands, British Columbia (no. 2008-12, 2008). Geological Survey of Canada, Vancouver, BC, Canada. 18 pp.